Stress analysis around a through crack in a thin copper film using molecular dynamics

Dan Johansson[1,a], Per Hansson[2,b] and Solveig Melin[3,c]

[1,2,3]Division of Mechanics, Department of Mechanical Engineering, Lund University, P.O. Box 118,

22100 Lund, Sweden

[a]dan.johansson@mek.lth.se, [b]per.hansson@mek.lth.se, [c]solveig.melin@mek.lth.se

Abstract. A small rectangular strip of FCC Cu, containing a through crack on the nano-scale subjected to loading under displacement control, is simulated using molecular dynamics. The geometry is chosen to mimic that of a thin film between two stiff layers and therefore the height of the strip is much smaller than the width. A plain strain situation is modeled by applying periodic boundary conditions in the direction of the crack front. The Lennard-Jones pair potential is used for the inter-atomic forces. The centrally placed crack is created by removing a few atoms inside the specimen. The crack is loaded perpendicular to the crack plane and comparisons with traditional linear elastic fracture mechanics concepts are made. The ultimate goal is to find a limit in model size beneath which linear elastic fracture mechanics measures looses their meaning.

Introduction

Technological advancements have provided means to design and manufacture components and structures on the nanometer scale with very high precision. Such components can be found in medical devices as well as in electromechanical circuits. One example within medicine is the use of small resonant beams, of length perhaps hundred micrometers but with cross section area measures about one micrometer, only, covered by a layer of a few nanometers in thickness. The layer is designed to detect specific biomarkers in the surrounding, and the concentration of such markers is detected through a shift in eigenfrequencies of the beam. Another common application is in nano-electro-mechanical systems, NEMS, where layers of thicknesses down to a few nanometers are designed for i.e. insulating or conductive purposes, or simply introduced to protect the component. We are thus in everyday life surrounded by structures whose behavior and function are determined from the atomistic level [1,2].

It is well established that structures with one or more spatial measures of a few nanometers, only, show material properties and behavior that differ from components at the macroscopic scale. This is due to factors such as the increasing number of surface atoms in relation to number of bulk atoms with decreasing size, and to the relatively lower dislocation density as compared to macroscopic structures. Also geometrical factors, such as crystal orientation, strongly influence the material properties; cf. e.g. [3,4].

Considering thin metallic layers, one difficulty lies in finding proper dimensioning rules that are scientifically based and commonly accepted among designers. One challenge lies in the prediction of sudden failure of the layer induced by mechanical loading. One critical failure mode is cracking. Even if the crack is small, of the length of a few nanometers only, it might jeopardize the

functionality of the coating and, eventually, extend to cause complete collapse of the component. Such unexpected events are, of course, necessary to understand and be able to predict. In this work, a thin strip of Cu, with height of only a few nanometers and holding a centrally placed crack loaded perpendicular to the crack plane through displacement control will be considered by molecular dynamics (MD) simulations using an in-house code. The results will be compared to traditional linear elastic fracture mechanics (LEFM) solutions to judge the impact of size of the geometry.

Problem specification
A thin strip of Cu, holding a centrally placed crack of length $2a$ along the x-direction according to Fig. 1 is studied. The crack is loaded perpendicular to the crack plane under displacement control. Coordinate directions (x, y, z) are shown in Fig. 1.
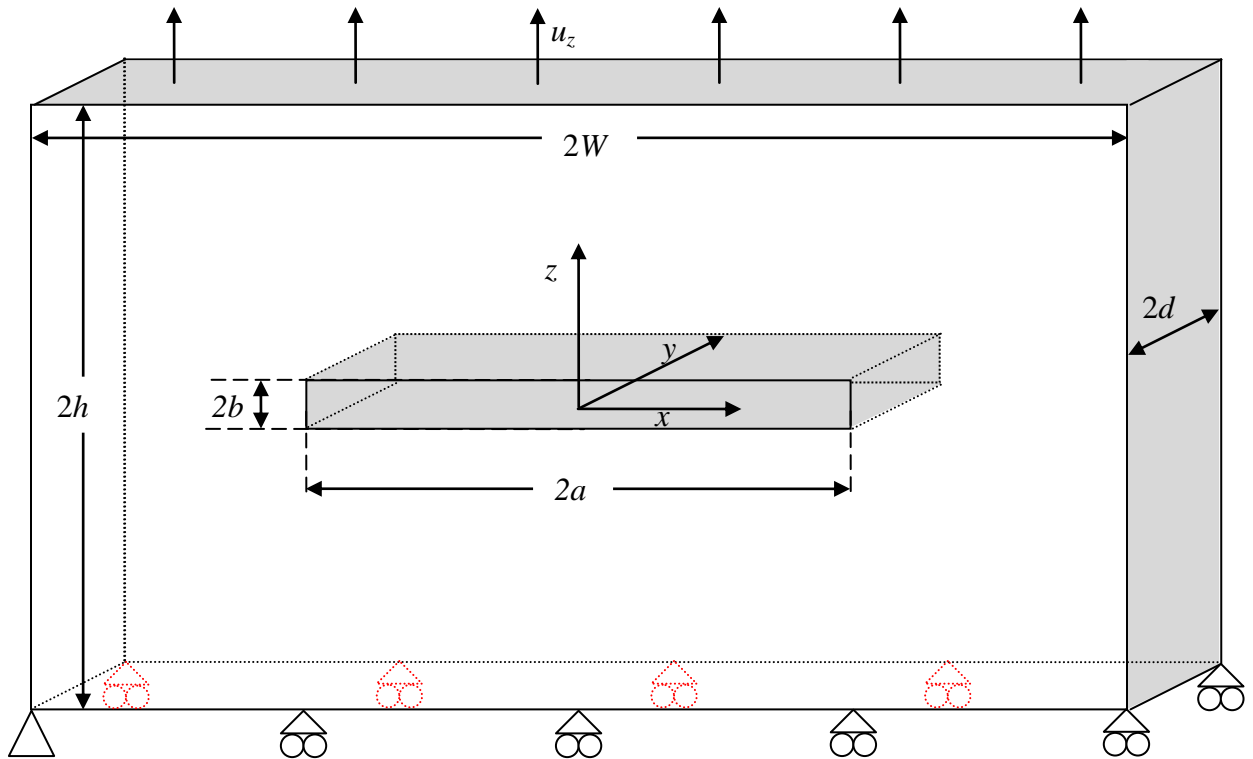

Fig.1. Model configuration. The crack is initially rectangular of size $2a$x$2b$.

The atomic arrangement in the strip is built from FCC Cu unit cells with lattice constant a_0. The height of the strip in the z-direction is $2h$, the width in the x-direction $2W$ and the thickness $2d$. The basic model comprises six unit cells in the y-direction so that $2d = 6a_0$. By imposing periodic boundary conditions in the y-direction, a state of plane strain is reached.

A crack is not naturally atomistically sharp and here the crack is introduced by removing a strip of height two unit cells along the crack line, giving a rectangular crack shape with length $2a$ and height $2b = 2a_0$. The boundary conditions at the bottom of the strip are realized by preventing movement of all atoms in the bottom atom layer in the z-direction, and furthermore lock the leftmost corner atom at the bottom atom layer in all directions. Displacement control is imposed by moving all atoms in

the two top atom layers at the top of the strip simultaneously at equal velocity in the [0 0 1]-direction. No boundary conditions are imposed at the sides of the strip.

Theory
Because of its computational simplicity, in this paper the Lennard-Jones 12-6 pair potential ϕ is employed, cf. [5]. The expression reads

$$\phi = 4\alpha \left[\left(\frac{\beta}{r} \right)^{12} - \left(\frac{\beta}{r} \right)^{6} \right] \tag{1}$$

In the Lennard-Jones expression the r^{-12}-term describes the electron orbital overlapping causing a short ranged repulsive force, the Pauli repulsion, while the r^{-6}-term describes the dispersion force which is a long ranged attracting force. The constants α and β in Eq. (1) are the depth of the potential well and the distance at which the inter-particle potential equals zero, respectively. The distance defined by β is also marks the length scale [5,6].

The Cauchy stress tensor $\boldsymbol{\sigma}$ for an atomistic ensemble region with volume V can be described as:

$$\boldsymbol{\sigma} = \begin{pmatrix} \sigma_{xx} & \sigma_{xy} & \sigma_{xz} \\ \sigma_{yx} & \sigma_{yy} & \sigma_{yz} \\ \sigma_{zx} & \sigma_{zy} & \sigma_{zz} \end{pmatrix} = -\frac{1}{2V} \sum_i \sum_{j \neq i} \boldsymbol{r}_{ij} \otimes \boldsymbol{f}_{ij} \tag{2}$$

Here $\boldsymbol{r}_{ij} = \boldsymbol{r}_j - \boldsymbol{r}_i$, where $\boldsymbol{r}_i$ and $\boldsymbol{r}_j$ denotes the positions for atom i and j, respectively, and

$$\boldsymbol{f}_{ij} = -\frac{\partial \phi(r_{ij})}{\partial r_{ij}} \frac{\boldsymbol{r}_{ij}}{r_{ij}} \tag{3}$$

with $r_{ij} = |\boldsymbol{r}_{ij}|$ [7]. The stresses calculated from Eq. (2) will be compared to linear elastic fracture mechanics solutions.

Simulation procedure
In this paper the results from two different geometries, G1 and G2, are presented, cf. Table 1. Each molecular dynamics simulation comprises three phases; problem setup, relaxation and loading.

During the problem setup phase all specific simulation parameters according to Table 1 are imposed. The atomic arrangement is generated, atoms are removed to form the crack and the boundary conditions are imposed at the bottom atomic layer.

In the second phase, the relaxation phase, the chosen temperature is assigned. This is done by multiplying the velocity of each atom with a scaling factor every two-hundred time step. Before the scaling factor is multiplied to the velocities of the atoms, it is updated. The magnitude of the scaling factor is determined by a Riemann sum of the mean value of the squared velocity. During the relaxation phase the strip in terms of size and volume moves towards a steady state, where the internal stress components only oscillate slightly around zero so that the relation between potential and kinetic energies keeps constant to a chosen magnitude. Further, during the relaxation, the top atomic layer is restricted so that this atomic layer remains plane and parallel with the xy-plane. This is imposed by initially putting all velocities equal to zero and then give all atoms in this atomic layer the same acceleration in the z-direction. This acceleration equals the mean of all these atoms accelerations in the z-direction.

After remaining at steady state for a few thousand time steps, the loading phase is entered and the two top atom layers are given a constant velocity in positive z direction causing the displacement, and, hence, the simulations are displacement controlled.

Material related parameters and temperature are given in Table 2. It should be noted that the present values of α, β, and r_C are not always chosen in other works. The present choice stems from [8] and provides a better agreement considering the Young's modulus E.

Table 1. Simulation parameters for geometries G1 and G2.

	G1	G2
Strip size $2Wx2h$ [unit cells]	80x20	20x10
Crack size $2ax2b$ [unit cells]	24x2	6x2
Number of atoms [-]	37248	4512
Total number of time steps [-]	48000	40000
Number of relaxation steps [-]	12000	8000
Strain rate [s^{-1}]	$1.14 \cdot 10^8$	$1.17 \cdot 10^8$
Final strain ε_{max} [%]	7.0	6.4
Time step [fs]	17	17
Temperature T [K]	0.001	0.001

Table 2. Material related parameters [8,9].

Lattice constant a_0 [nm]	0.36
Young's modulus E [GPa]	110
Poisson's ratio ν [-]	0.34
Potential well depth α [eV]	0.1515
Distance for zero potential β [nm]	0.2338
Cut-off radius r_C [nm]	$2.74\,\beta = 0.6406$

Results and Discussion

Both geometries were initially relaxed, and both were reduced in volume due to the relaxation; G1 by 6.4% and G2 by 6.8%. In the z-direction the height was reduced by approximately 3.2% for both geometries. From this relaxed stage, loading was pursued until a maximum strain, ε_{max}, cf. Tabel 1, was reached. At this point the atomic arrangements still behaved elastic, with no signs of plasticity in terms of dislocation formation.

In Fig. 2 the stresses σ_{zz} and σ_{zx} for geometry G1 are shown at maximum strain ε_{max}. Fig. 2a and Fig. 2c show the results from the MD simulation and Fig. 2b and Fig. 2d are the LEFM solutions for an infinitely sharp crack in a displacement loaded finite strip as taken from [10]. The stresses in Fig. 2b and Fig. 2d are shown with the exclusion of an area of height $2a_0$ around the crack, marked by a line, in similarity to Fig. 2a and Fig. 2c from the MD simulation. Note that the length scales differ between the plots of the MD and LEFM results, and in Fig. 2a and Fig. 2c the areas for which the linear elastic solutions in Fig. 2b and Fig. 2d are presented, are framed. Also note that for the MD simulation, the entire height of the strip, $2h$, is displayed. Further, in Fig. 3, σ_{zz} ahead of the crack

tip and just below the crack line, taken from Fig. 2a and Fig. 2c, are drawn. Corresponding results for geometry G2 are found in Fig. 4 and Fig. 5.
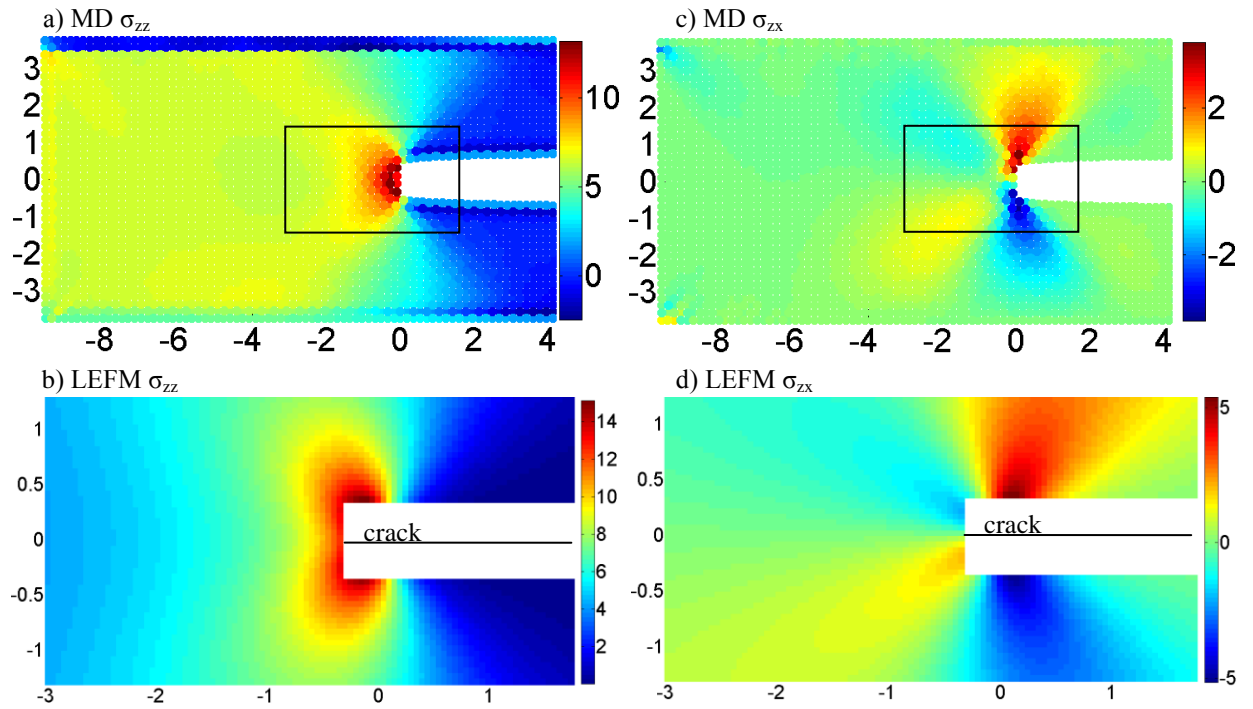

Fig.2. σ_{zz} and σ_{zx} for the left half of geometry G1. Abscissa and ordinate are given in [nm]. The bars are in [GPa] a) and c): MD simulations. b) and d): LEFM solutions.
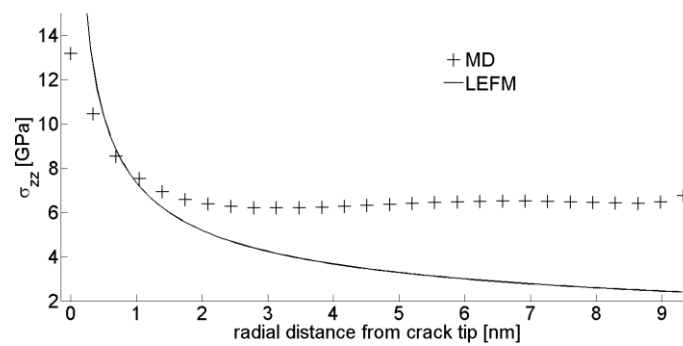

Fig.3. σ_{zz} ahead of the crack tip for G1. The abscissa is in [nm] and the ordinate in [GPa]. + show MD result for the atoms just below $z = 0$ and the solid line is the LEFM solution.
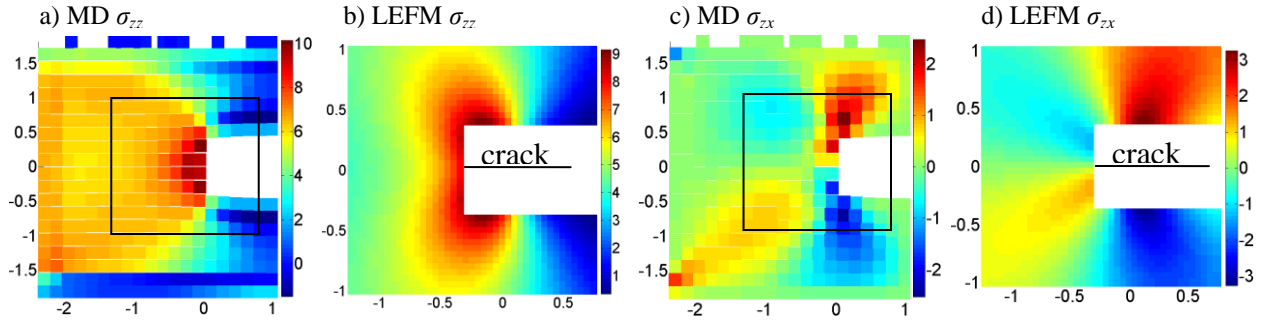
Fig.4. σ_{zz} and σ_{zx} for the left half of geometry G2. Abscissa and ordinate are given in [nm]. The bars are in [GPa] a) and c): MD simulations. b) and d): LEFM solutions.
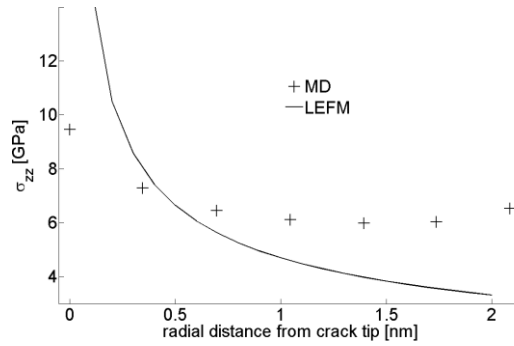

Fig.5. σ_{zz} ahead of the crack tip for G2. The abscissa is in [nm] and the ordinate in [GPa]. + show MD result for the atoms just below $z = 0$ and the solid line is the LEFM solution.

First consider the results concerning the largest geometry, G1, in Fig. 2 and Fig. 3. For σ_{zz}, in general terms judging from Fig. 2, the stress fields agree in shapes, magnitude and trends between the MD simulation and the LEFM solution. The stress levels of σ_{zz} as obtained from the MD (+) and LEFM ($-$) calculations are seen in Fig. 3. Of course, the sharp crack gives higher stress levels than the rectangular shaped crack. Another fact contributing to the difference between the LFEM and the simulated stress is that the atoms z-coordinate is not exactly equal to zero. Studying Fig. 2 again, for σ_{zx} the stress fields agree very well in shape, magnitude and trend between the MD simulation and the LEFM solution. The deviations seen in Fig. 3 and Fig. 5 is explained by the fact that LEFM only describes stress contributed by the crack while in the simulations a stress in the z-direction σ_{zz} is introduced in the strip due to tensile strain ε_{zz}. This argumentation is proven by that the shear stress σ_{zx} fields for the simulations and the LEFMs don not show the same magnification difference far from the crack tips.

Further it is seen from Fig. 2a that the boundary is affecting the σ_{zz} stress distribution relatively far ahead of the crack front, raising the stress level as compared to the LEFM solution in Fig. 2b.

Turning to the smaller geometry G2 in Fig. 4 and Fig. 5, it is noticed that all effects found for G1 are enhanced for G2. Still there is a resemblance between the MD and LEFM stress fields, but the inference from the boundaries have increased significantly.

Conclusions
Molecular dynamics simulations have shown that cracked layers of small enough size react differently than macroscopic components upon loading. In this investigation, displacement controlled loading of cracked layers of Cu, with layer thicknesses less than a nanometer, were considered. The stress fields obtained from the MD simulations were compared to LEFM continuum solutions close to the crack front.

The stress fields as determined from MD and LEFM continuum solutions were, shown to increasingly deviate as the layer thickness decreased. Even so, the general appearances of the stress distributions were kept. The influence from boundaries increased markedly as the layer thickness decreased. This becomes obvious when comparing Fig. 2c, where the shear stress field spreads as in LEFM, and Fig. 4c, where the shear stress field is drawn towards the corners. Hence, LEFM will give a good approximation but due to boundary effects the LEFM result will only be able to describe the general shapes of the stress fields and give an idea of the stress magnitudes for the atoms that are very near the crack tip.

References
[1]   B. Ilic, Y. Yang and H.G. Craighead: Virus detection using nanoelectromechanical devices, J. Appl. Phys. Vol 85-2604 (2004)
[2]   D.H. Reich, M. Tanase, A. Hultgern, L.A. Bauer, C.S. Chen et al.: Biological applications of multifunctional magnetic nanowires, J. Appl. Phys. Vol. 93-7275 (2003)
[3]   P. Olsson, S. Melin and C. Persson: Atomistic simulations of tensile and bending properties of single-crystal bcc iron nanobeams, Phys. Rev. B 76, 224112 (2007)
[4]   P. Olsson and S. Melin, in *Atomistic studies of the elastic properties of metallic BCC nanowires and films*, edited by R Pyrz and J C Rauhe IUTAM Symposium on Modelling Nanomaterials and Nanosystems (2008), p.221-230
[5]   J.E. Jones: On the Determination of Molecular Fields, Proc. R. Soc. Lond. A Vol. 106 (1924), p. 463-477
[6]   D.C. Rapaport: The Art of Molecular Dynamics (Cambridge University Press, UK 2004).
[7]   M. Zhou: A new look at the atomic level virial stress: on continuum-molecular system equivalence, Proc. R. Soc. Lond. A Vol 459 (2003), p. 2347-2392
[8]   G. Ziegenhain, A. Hartmaier and H.M. Urbassek: Pair vs many-body potentials: Influence on elastic and plastic behavior in nanoindentation of fcc metals, J. Mech Phys. Solids Vol. 57, 1514-1526, (2009)
[9]   D.R. Askeland: The Science and Engineering of Materials (Chapman & Hal,l UK/China 1996).
[10] M. Isida: Effect of width and length on stress intensity factors of internally cracked plates under various boundary conditions, Int. J. Fract. Mech. 7 (1971) p 301.